# *Prediction of Stability of Underground Openings Using EMM*


***Anupam Mital***
*&*
***VK Arora***

*Department of Civil Engineering,*
*National Institute of Technology,*
*Kurukshetra – 136 119, India*
*Phone: +91 1744 239993*

## ABSTRACT

Excavation of underground openings disturbs the state of equilibrium of stresses existing in a rock mass and causes their redistribution. For the design of an underground opening, prediction of its stability is the most important aspect. Amongst the various methods for their evaluation, EMM (equivalent material modelling) has an advantage of providing a physical feel of both the qualitative and quantitative understanding of the problem.

After developing suitable equivalent materials and preparation of models on selection of equivalent material compositions, the effect of height of overburden on stability of openings in stratified formation for rectangular openings has been studied.

The effect of height of overburden on limiting span of roof has been reported in the paper. The studies led to development of proper understanding of the ground response above an opening, well in advance, for the formation under consideration.

***Keywords:*** Equivalent material model, Underground Opening, Stability

## 1. INTRODUCTION

The various factors affecting the stability of underground openings are the strength and the deformational characteristics of the rock mass, the in-situ state of stresses, the size and shape of the opening, the method and sequence of excavation, the rate of advance, the method of support and the water conditions, if any. Review of literature for the prediction of stability revealed that the designers and researchers have often restricted themselves to analytical, numerical and empirical methods requiring special assumptions, mathematical simplifications, statistically large database, providing lesser informations when applied to complex geological formations.

A laboratory study of the effect of overburden on stability in horizontally stratified formations is reported in this paper.

Using EMM (equivalent material modelling), the work comprised of developing suitable equivalent model materials, modelling technique involving design of the equivalent formation, construction and testing of several models, adopting a geometrical scale of 1:50.

These studies enabled to evolve empirical relationships for the estimation of roof deformations and to find out the status of stability of an underground opening from non-dimensional plots and prediction of stable roof span.

This could be of significant help to the practicing engineers in the stability analysis and optimizing recovery of precious minerals.

The developed empirical relationships and non-dimensional plots have been applied to various tunnelling and mining projects and the results compared with the values obtained from actual observations and beam theory, in order to establish their applicability in the field.

## 2. EQUIVALENT MATERIAL MODELLING (EMM)

Equivalent material modelling technique is based upon dimensional analysis and similitude. It provides an effective means for imitating a specific real situation. Here, the qualitative and quantitative analysis of underground openings can be ascertained. The post-failure behaviour of the rock mass surrounding the opening can also be very well ascertained (Bieniawski,1984 and Singh et al.,1985).

In order to achieve best comparable results with the prototype, selection of artificial equivalent materials, model construction and model workings have to be performed faithfully.

## 3. PHYSICO-MECHANICAL ROPERTIES OF MODEL MATERIALS

For developing suitable equivalent model materials, 46 mixes of plaster of Paris, fine sand and mica powder were investigated. The prismatic specimens prepared from these mixes were tested for compressive strength, tensile strength both along and across the axis and flexural strength along with determination of density. The results of these tests on various EM compositions provided a wide range of equivalent materials with their mean values arrived at after testing 5 to 6 samples for each test (Table 1). The density of EM compositions varied from 770 kg/m$^3$ to 1190 kg/m$^3$. The compressive strength varied from 94.736 kPa to 542.131 kPa. Tensile strength along the axis varied from 24.812 kPa to 103.366 kPa and across the axis varied from 20.104 kPa to 127.687 kPa. The flexural strength varied from 83.163 kPa to 245.763 kPa.

Table 1- Physico-mechanical properties of equivalent materials

| EM composition code | POP/Sand/ Mica % volume | UN or N | Density $\rho_m$ kg/m$^3$ | Compressive strength $(\sigma_c)_m$ kPa | Tensile strength kPa | | Flexural strength $(\sigma_f)_m$ kPa |
|---|---|---|---|---|---|---|---|
| | | | | | Along the axis $(\sigma_{t1})_m$ | Across the axis $(\sigma_{t2})_m$ | |
| I-A | 15/30/55 | UN | 771 | 152.401 | 27.558 | 44.328 | 102.875 |
| | | N | | 94.736 | 24.812 | 21.968 | (83.163) |
| I-B | 15/35/50 | UN | 830 | 172.113 | 29.225 | 44.916 | 105.327 |
| | | N | | 111.898 | 25.302 | 22.360 | (83.163) |
| I-C | 15/40/45 | UN | 880 | 190.354 | 31.088 | 45.701 | 107.779 |
| | | N | | 126.608 | 25.890 | 22.752 | (83.163) |
| I-D | 15/45/40 | UN | 921 | 183.783 | 33.540 | 46.289 | 132.395 |
| | | N | | 132.983 | 28.146 | 26.185 | 100.326 |
| I-E | 15/50/35 | UN | 1000 | 176.232 | 37.365 | 47.858 | 156.520 |
| | | N | | 141.123 | 31.382 | 29.813 | 120.038 |
| I-F | 15/55/30 | UN | 1030 | 200.651 | 41.680 | 48.250 | 169.367 |
| | | N | | 145.928 | 30.794 | 24.714 | 115.134 |
| I-G | 15/60/25 | UN | 1080 | 227.817 | 44.033 | 48.741 | 176.722 |
| | | N | | 149.459 | 29.323 | 23.145 | 107.779 |
| I-H | 15/65/20 | UN | 1121 | 212.420 | 42.268 | 46.387 | 169.367 |
| | | N | | 149.066 | 27.656 | 20.889 | 102.875 |
| I-I | 15/70/15 | UN | 1149 | 200.847 | 40.993 | 44.426 | 162.012 |
| | | N | | 148.968 | 25.792 | (20.104) | 85.615 |
| II-A | 20/30/50 | UN | 829 | 219.383 | 49.623 | 66.001 | 168.877 |
| | | N | | 146.026 | 47.858 | 46.191 | 107.289 |
| II-B | 20/35/45 | UN | 881 | 226.247 | 51.781 | 66.688 | 174.270 |
| | | N | | 159.462 | 47.270 | 43.249 | 114.644 |
| II-C | 20/40/40 | UN | 919 | 227.326 | 53.546 | 67.178 | 178.684 |
| | | N | | 170.544 | 45.995 | 40.405 | 119.547 |
| II-D | 20/45/35 | UN | 1001 | 321.572 | 55.998 | 77.573 | 187.314 |
| | | N | | 213.204 | 49.231 | 40.797 | 120.038 |
| II-E | 20/50/30 | UN | 1029 | 382.179 | 56.979 | 81.594 | 194.767 |
| | | N | | 229.778 | 51.291 | 36.678 | 115.134 |
| II-F | 20/55/25 | UN | 1080 | 436.706 | 58.940 | 86.400 | 201.926 |
| | | N | | 239.977 | 50.212 | 40.601 | 120.528 |
| II-G | 20/60/20 | UN | 1120 | 487.212 | 60.607 | 90.322 | 209.281 |
| | | N | | 247.823 | 48.643 | 44.230 | 125.530 |
| II-H | 20/65/15 | UN | 1151 | 457.300 | 60.117 | 88.949 | 204.378 |
| | | N | | 247.136 | 46.877 | 43.935 | 120.528 |
| II-I | 20/70/10 | UN | 1190 | 418.661 | 59.627 | 86.694 | 199.671 |
| | | N | | 246.254 | 45.308 | 42.170 | 115.625 |
| III-A | 25/40/35 | UN | 1030 | 472.795 | 91.401 | 122.391 | 230.465 |
| | | N | | 315.295 | 82.183 | 81.006 | 209.281 |
| III-B | 25/45/30 | UN | 1079 | 523.988 | 97.384 | 125.530 | 236.839 |
| | | N | | 338.243 | 81.006 | 76.102 | 186.627 |
| III-C | 25/50/25 | UN | 1120 | 542.131 | 103.366 | 127.687 | 245.763 |
| | | N | | 361.192 | 76.004 | 70.218 | 168.386 |
| III-D | 25/55/20 | UN | 1150 | 528.793 | 99.345 | 126.805 | 231.445 |
| | | N | | 352.758 | 74.337 | 68.747 | 141.809 |
| III-E | 25/60/15 | UN | 1191 | 515.848 | 95.422 | 125.726 | 214.185 |
| | | N | | 343.833 | 73.062 | 67.080 | 108.760 |

*Notations:* UN = unnotched sample; N = notched sample with 8 minutes delay in notching

## 4. DEVELOPMENT OF MODELLING TECHNIQUE

Using equivalent material modelling technique, it was intended to have a better physical feel of the problem by considering simple rectangular opening through an actual field stratified formations of a Colliery in Jharia coal field, Bihar.

The work comprised of developing suitable equivalent model materials for preparation of prismatic specimens of varying strengths. A weakening coefficient of 0.5 was arrived at after testing of a preliminary model. Using Buckingham – Pi dimensional relationship incorporating weakening coefficient, equivalent strengths were calculated using the following equation known as designing equation.

$$\sigma_m = \alpha_L . K . \frac{\rho_m}{\rho_p} . \sigma_p \qquad (1)$$

where

$\sigma_m$ = model material strength in kPa,
$\alpha_L$ = geometrical scale,
K = weakening coefficient,
$\rho_m$ = density of model material in kg/m$^3$,
$\rho_p$ = density of proto material in kg/m$^3$ and
$\sigma_p$ = proto material strength in kPa.

Thereafter, equivalent material compositions were selected for model simulation of the proto formation and laid in layers after working out the quantities of various ingredients per layer, in a model frame of size 3.00 m × 1.80 m × 0.25 m specially designed and fabricated for the purpose.

In all, four models of size 3.00 m × 1.17 m × 0.25 m were prepared (Fig. 1). A part of the overburden (38.5 m) was simulated in these models above the proposed opening, i.e. roof level. For the remaining rock mass above the overburden simulated, the overburden height was simulated by applying required surcharge pressures on the top of the formation to bring the opening under the influence of desired height of overburdens. The models were instrumented using LVDTs for the measurement of deformations.

## 5. TESTING OF MODELS

Four models were tested for roof deformational behaviour for heights of overburden above the opening of 5600 mm, 4200 mm, 2800 mm and 1400 mm corresponding to proto overburdens of 280 m, 210 m, 140 m and 70 m respectively till failure, varying the width of the opening.

The roof deformations were measured at various monitoring points fixed along rows and columns above the opening (Fig. 2). Deformations were measured before and after every excavation stage and also during the equivalent cycle of operation of 4 cm per 30 minutes in the model corresponding to the normal operational cycle of 2 m per

3 hours and 30 minutes in the field. Here, prominent phenomena were observed visually (Fig. 3) and recorded photographically at frequent intervals.

## 6. RESULTS AND DISCUSSION

### 6.1 Effect of Overburden on Deformation of Roof

A comparison of deformations recorded by LVDT No. 1 positioned 20 mm above the roof along the centre line of opening, is presented in Table 2 and Fig. 4 for various models tested under different heights of overburden. The interpretation of test results (Table 2) and test plot (Fig. 4) reveals that the deformation increases with increase in overburden height, for all widths of opening. The percentage increase in deformation with percentage increase in overburden height for a given width of opening of 240 mm is as follows:

(i) 100 % increase in overburden height increases deformation by 170.19 %.
(ii) 200 % increase in overburden height increases deformation by 275.00 %.
(iii) 300 % increase in overburden height increases deformation by 382.69 %.

Further,

(i) 100 % increase in overburden height increases deformation by 170.19 %.
(ii) Subsequent 100 % increase in overburden height further increases deformation by 38.79 %.
(iii) Further subsequent 100 % increase in overburden height further increases deformation by 28.72 %.

Table 2 - Deformations measured at monitoring point 1 for various overburden heights

| Model | Overburden height $H_m$, mm | Deformation mm at LVDT No. 1 | | | | | | | | | |
|---|---|---|---|---|---|---|---|---|---|---|---|
| | | Width of opening, mm | | | | | | | | | |
| | | 80 | 120 | 160 | 200 | 240 | 280 | 300 | 320 | 340 | 360 |
| 3 | 1400 | 0.01 | 0.09 | 0.31 | 0.62 | 1.04 | 1.56 | - | 2.74 | - | 4.09 |
| 2 | 2800 | 0.11 | 0.42 | 0.90 | 1.60 | 2.81 | 5.96 | - | 6.68 | O.O.R. | O.O.R. |
| 5 | 4200 | 0.24 | 0.54 | 1.30 | 2.22 | 3.90 | 6.69 | - | O.O.R. | O.O.R. | O.O.R. |
| 1 | 5600 | 0.35 | 0.68 | 1.51 | 2.85 | 5.02 | 7.42 | O.O.R. | O.O.R. | O.O.R. | O.O.R. |

The percentage variation of increase of deformation with overburden height (1400 mm onwards) is shown in Fig. 5. From the figure, it is observed that for a given width of opening, the increase of deformation decreases with increase in overburden height and the curve finally becomes asymptotic. At this stage, the results are in line with the beam theory, as per which, the deformation of the roof is independent of the height of overburden above the opening. Similar behaviour was observed for all other widths of opening.

### 6.2 Effect of Overburden on Stability

To study the effect of height of overburden ($H_m$) on stability, a comparison of stable width of opening ($w_m$) or limiting span of roof is presented in Table 2 and Fig. 6 for various models tested under different heights of overburden. From the table and figure, it is observed that the limiting span of the roof decreases with increase in overburden height. The percentage decrease in the limiting span of roof with percentage increase in overburden height (1400 mm onwards) is as follows:

(i) 100 % increase in overburden height decreases the limiting span of roof by 15.00 %.
(ii) 200 % increase in overburden height decreases the limiting span of roof by 22.50 %.
(iii) 300 % increase in overburden height decreases the limiting span of roof by 25.00 %.

Further,

(i) 100 % increase in overburden height decreases the limiting span of roof by 15.00 %.
(ii) Subsequent 100 % increase in overburden height further decreases the limiting span of roof by 8.82 %.
(iii) Further subsequent 100 % increase in overburden height further decreases the limiting span of roof by 3.23 %.

The percentage variation of decrease in limiting span of roof with overburden height (1400 mm onwards) is shown in Fig. 7. From the figure, it is observed that decrease in the limiting span of roof decreases with increase in overburden height and the curve finally becomes asymptotic. At this stage, the results are again in line with the beam theory, as per which, the limiting span of roof is independent of the height of overburden above the opening.

### 6.3 Comparison of Predicted and Observed Roof Spans for Stability

The observed stable roof spans for the four overburdens are compared with the values of predicted roof spans, applying beam theory to the models using the following equation:

$$L = \sqrt{\frac{2\sigma_t Kt}{\gamma}} \qquad (2)$$

The predicted stable roof spans are quite close to their observed values in the models. In calculating the predicted roof spans using beam theory, the following assumptions have been considered.

(i) to be conservative, the horizontal stress ($\sigma_h$) acting on the beam is taken as zero.

(ii) under the overburden pressure, the roof strata is solidly clamped at the side walls and is considered to behave like fixed or ideal beam.

Using beam theory for the models 4,3, 2 and 1,

Here, $\sigma_t$ = 21.968 kPa = 21968 Pa = 21968 N/m$^2$
t = 40 mm = 0.04 m
$\gamma$ = $771 \times 9.807$ N/m$^3$
K = 0.5

$\therefore$ Limiting span $L = \sqrt{\frac{2 \times 21968 \times 0.5 \times 0.04}{771 \times 9.807}}$
= 0.341 m
= 341 mm

The observed stable roof spans for the above four models are compared with the predicted stable roof span using beam theory and the percentage variation is as under:

Table 3 – Percentage variation of observed and predicted stable roof span

| Model | Overburden, kN/m$^2$ | Observed stable roof span, mm | Predicted stable roof span, mm | Variation % |
|---|---|---|---|---|
| 4 | 14.763 | 400 | 341 | 14.75 |
| 3 | 29.526 | 340 | 341 | 00.29 |
| 2 | 44.289 | 310 | 341 | 10.00 |
| 1 | 59.052 | 300 | 341 | 13.67 |

Hence, the predicted stable roof spans are quite close to the observed stable roof spans. The decrease in the observed stable roof spans with increase in overburden can be attributed to the fact that a mine roof, even if resolved to an equivalent beam, differs from a fixed-end, self-loaded beam as it always carries a load of the overlying mass until delamination due to differential deflection. By that time, the tensile strength drops to a certain residual value (Singh, 1991).

Hence, the limiting span (L) is a function of overburden ($P_o$ or $\gamma H$) alongwith other parameters such as tensile strength ($\sigma_t$), thickness of the layer (t), weakening coefficiant (K) and the unit weight of the layer ($\gamma$), i.e.

$$L = f(P_o, \sigma_t, t, K, \gamma) \quad (3)$$

An attempt was made to establish a relation between the limiting span (L) with $P_o$, $\sigma_t$, t, K and $\gamma$ and the following relation was established (Mittal, 2000):

$$L = 1.7664 \sqrt{\frac{\sigma_t K t}{\gamma}}\, e^{-6.0 \times 10^{-6} P_o} \quad (4)$$

where L is in metres, $P_o$ is in N/m$^2$, $\sigma_t$ is in N/m$^2$, t is in metres and $\gamma$ is in N/m$^3$.

The limiting span from above equation has been found to be close to the actual values with in permissible limits of variation. Hence, it may be applied in the field using a safety factor to cover unforeseen geological defects in the roof.

## 7. CONCLUSION

EMM studies on underground openings led to the development of proper understanding of the ground response above an opening, well in advance, for the formation under consideration. The developed relationship could be of help in the design of the actual opening. These might act as guidelines, in simple terms, particularly for underdeveloped areas where underground excavations are still being carried out on traditional lines in unscientific and haphazard manner. EMM, though labour intensive, is economical and will constitute a very small percentage of the project cost. This will help in minimising ground control hazards while at the same time maximising recovery at an acceptable cost.

### *Reference*

Bieniawski, Z.T. (1984). Rock Mechanics Design in Mining and Tunnelling, A.A. Balkema, Rotterdam, The Netherlands.

Singh, T.N. and Farmer, I.W. (1985). A Physical Model of an Underground Coal Mine Prototype. Mining Engineering, Vol. 3, pp.319-326.

Singh, T.N. (1991). Underground Winning of Coal. Oxford and IBH, New Delhi, India.

Mittal, Anupam (2000). Model Studies on Underground Openings in Stratified Rocks, Ph.D. Thesis, Kurukshetra University, Kurukshetra, India.

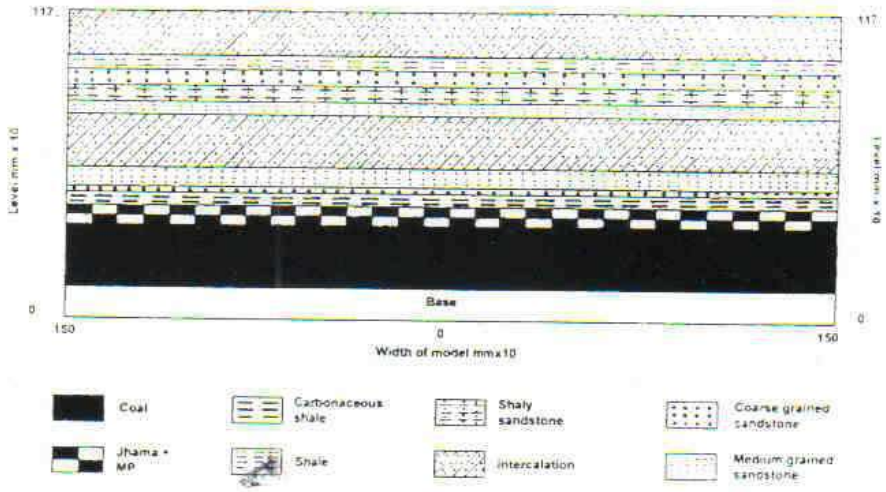


Fig. 1 – View of completed model

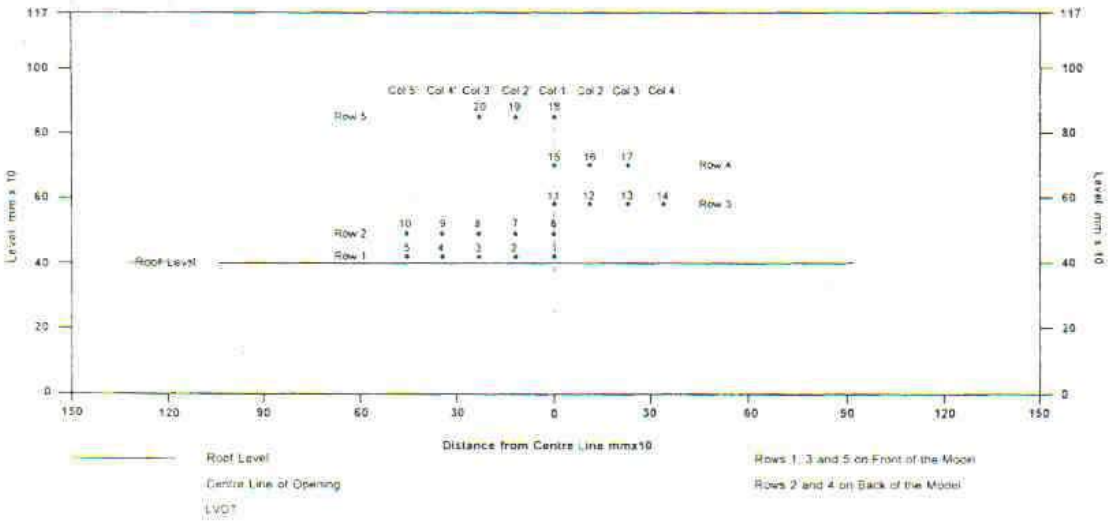


Fig. 2 – Configuration of monitoring points for Model 1

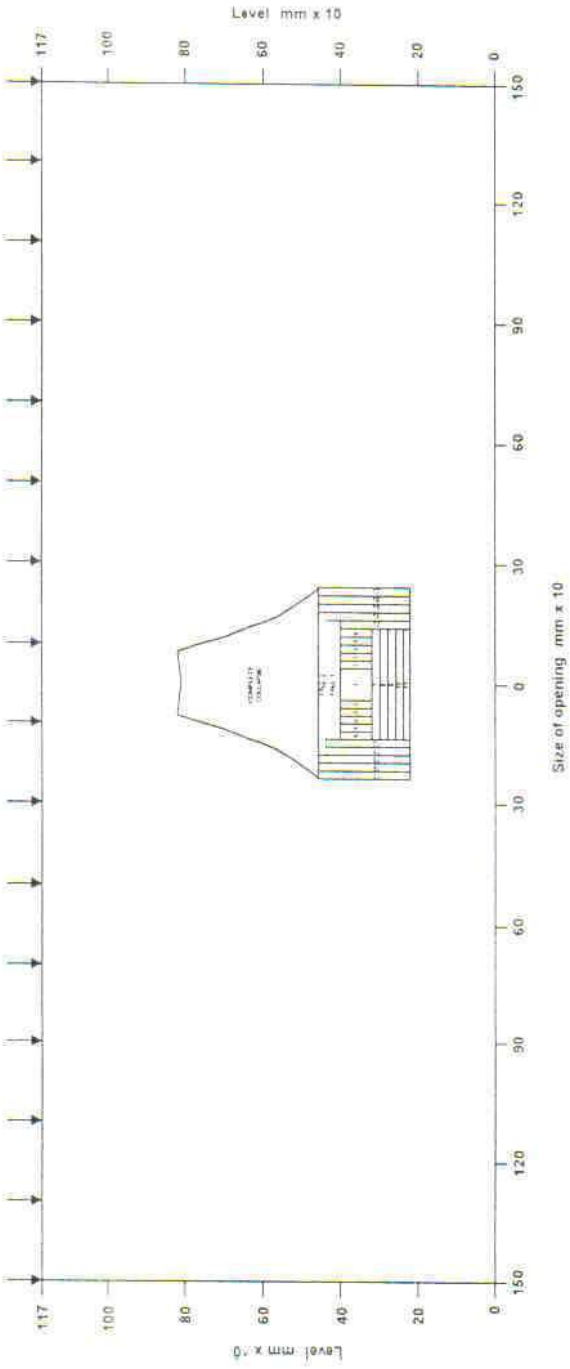


Fig. 3 – Excavation stages and roof falls in Model 1

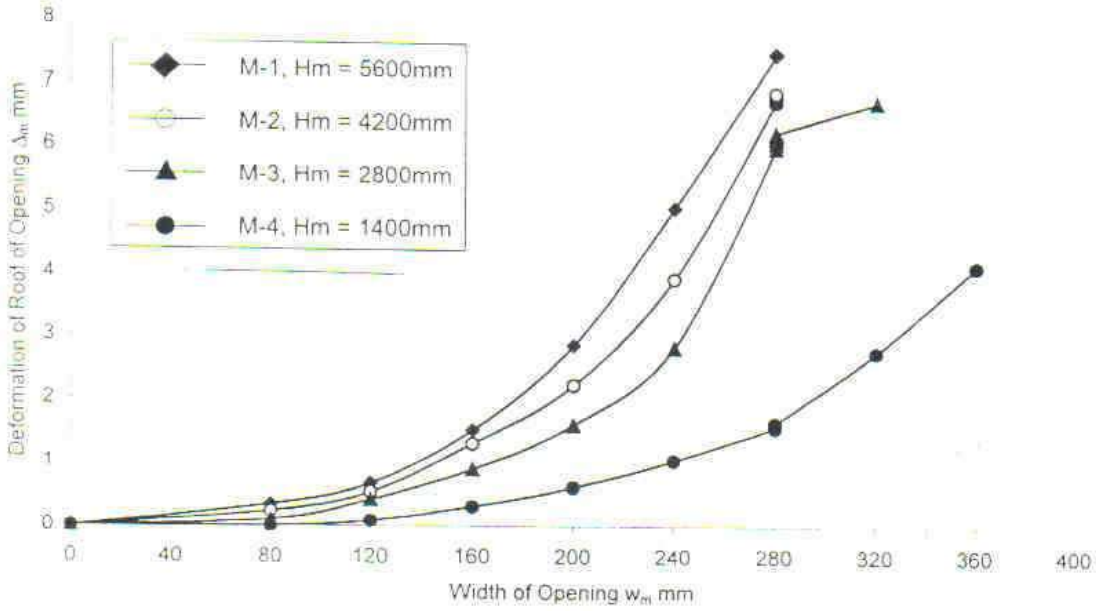


Fig. 4 – Comparison of deformations recorded by LVDT 1, positioned 20mm above the opening along the centre line of opening

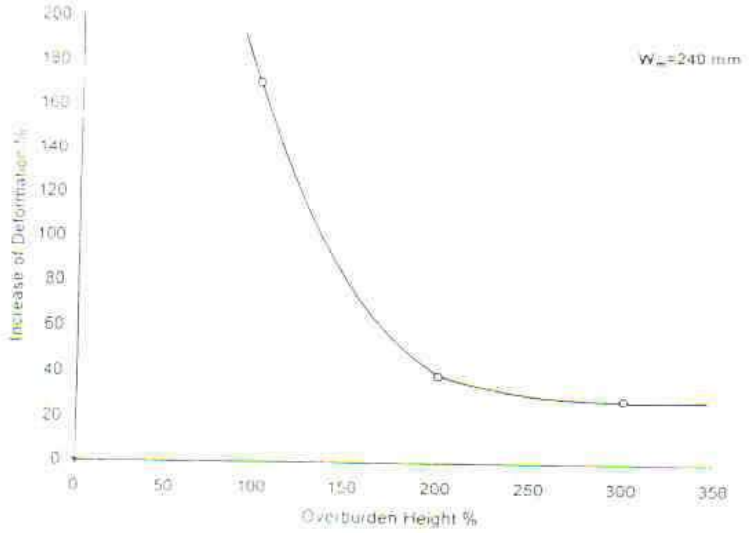


Fig. 5 – Per cent variation of increase of deformation of roof of opening with overburden height

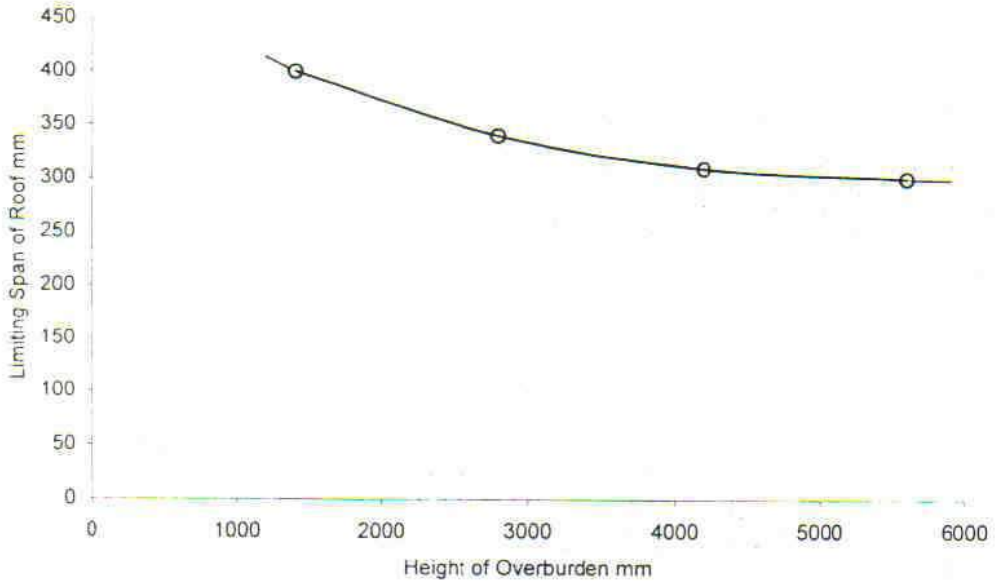


Fig. 6 – Variation of limiting span of roof with height of overburden

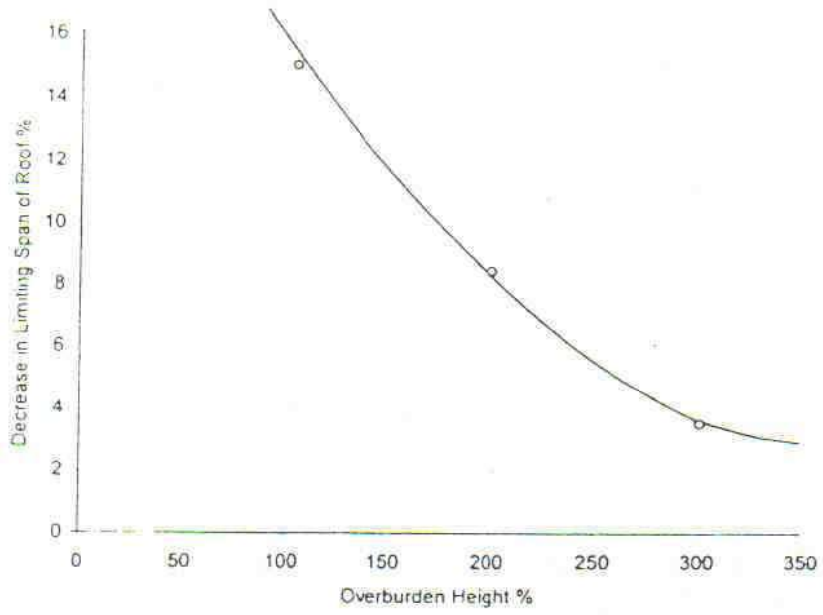


Fig. 7 – Variation of decrease in limiting span of roof with overburden height